The American Journal of Pathology, Vol. 180, No. 6, June 2012

http://dx.doi.org/10.1016/j.ajpath.2012.02.012

Stem Cells, Tissue Engineering, and Hematopoietic Elements

Presenilin-1 L166P Mutant Human Pluripotent Stem Cell–Derived Neurons Exhibit Partial Loss of γ-Secretase Activity in Endogenous Amyloid-β Generation

Philipp Koch,*† Irfan Y. Tamboli,‡ Jerome Mertens,* Patrick Wunderlich,‡ Julia Ladewig,* Kathrin Stüber,*† Hermann Esselmann,§ Jens Wiltfang,§ Oliver Brüstle,*† and Jochen Walter‡

From the Institute of Reconstructive Neurobiology, LIFE & BRAIN Center, University of Bonn and Hertie Foundation; LIFE & BRAIN GmbH†; and the Department of Neurology,‡ University of Bonn, Bonn; and the Laboratory for Molecular Neurobiology,§ Department of Psychiatry and Psychotherapy, University of Duisburg-Essen, Essen, Germany*

Alzheimer's disease (AD) is the most frequent cause of dementia. There is compelling evidence that the proteolytic processing of the amyloid precursor protein (APP) and accumulation of amyloid-β (Aβ) peptides play critical roles in AD pathogenesis. Due to limited access to human neural tissue, pathogenetic studies have, so far, mostly focused on the heterologous overexpression of mutant human APP in non-human cells. In this study, we show that key steps in proteolytic APP processing are recapitulated in neurons generated from human embryonic and induced pluripotent stem cell–derived neural stem cells (NSC). These human NSC-derived neurons express the neuron-specific APP_{695} splice variant, BACE1, and all members of the γ-secretase complex. The human NSC-derived neurons also exhibit a differentiation-dependent increase in Aβ secretion and respond to the pharmacotherapeutic modulation by anti-amyloidogenic compounds, such as γ-secretase inhibitors and nonsteroidal anti-inflammatory drugs. Being highly amenable to genetic modification, human NSCs enable the study of mechanisms caused by disease-associated mutations in human neurons. Interestingly, the AD-associated $PS1_{L166P}$ variant revealed a partial loss of γ-secretase function, resulting in the decreased production of endogenous Aβ40 and an increased Aβ42/40 ratio. The $PS1_{L166P}$ mutant is also resistant to γ-secretase modulation by nonsteroidal anti-inflammatory drugs. Pluripotent stem cell–derived neurons thus provide experimental access to key steps in AD pathogenesis and can be used to screen pharmaceutical compounds directly in a human neuronal system. *(Am J Pathol 2012, 180:2404–2416; http://dx.doi.org/10.1016/j.ajpath.2012.02.012)*

Alzheimer's disease (AD) is characterized by progressive neuronal loss and the accumulation of amyloid β-peptides (Aβ) in the form of extracellular plaques.[1] Aβ is produced from the larger amyloid precursor protein (APP) by a sequential proteolytic processing cascade.[2] Due to alternative splicing, several mRNA variants of APP are described. While the 751 and 770 amino acid–long splice variants of APP are found in most tissues, a shorter, 695 amino acid–long splice variant is selectively expressed in human neurons.

The generation of Aβ includes the initial cleavage of APP by the β-secretase BACE1, an aspartic protease highly expressed in neuronal cells, but also at lower levels in non-neuronal cells and tissues.[3] Accordingly, neurons produce

Supported by the German Federal Ministry for Education and Research (BioPharma-NeuroAllianz grants 0315608A, 0315608B), the German Research Foundation (SFB645, KFO177), the European Commission (grant 222943, NeuroStemCell), the Hertie Foundation, and by the grant PURE (Protein Research Unit Ruhr within Europe) from the State Government North Rhine-Westphalia.

Accepted for publication February 9, 2012.

P.K., I.Y.T., and J.M. contributed equally to this work.

Disclosure: O.B. is a co-founder of and has stock in Life & Brain GmbH.

Supplemental material for this article can be found at *http://ajp.amjpathol.org* or at *http://dx.doi.org/10.1016/j.ajpath.2012.02.012*.

Current address of I.Y.T., Department of Neuroscience, Georgetown University, Washington, DC.

Address reprint requests to Jochen Walter, Ph.D., Molecular Cell Biology, Department of Neurology; or Oliver Brüstle, Ph.D., Institute of Reconstructive Neurobiology, Life & Brain Center, University of Bonn, Sigmund-Freud-Str., 53127 Bonn, Germany. E-mail: jochen.walter@ukb.uni-bonn.de or brustle@uni-bonn.de.

higher amounts of Aβ as compared to other cell types. The cleavage of APP by BACE1 occurs at the N-terminus of the Aβ domain and results in the secretion of the soluble APP ectodomain (sAPP-β) and a membrane-tethered C-terminal fragment (APP-CTF) containing the Aβ sequence. APP-CTFs generated by BACE1 can be further cleaved by γ-secretase, a high molecular weight complex consisting of presenilins (PS) as the catalytic moieties and at least three additional components called Nicastrin, anterior pharynx-defective 1 (Aph-1), and presenilin enhancer 2 (Pen-2).[4] The cleavage of APP-CTFs by γ-secretase is heterogeneous, resulting in the production of different Aβ length variants including Aβ42, Aβ40, and Aβ38.[5,6] The prevailing view of AD pathogenesis is that accumulation and aggregation of Aβ peptides, particularly of Aβ42, is a critical event in the pathogenesis of AD.[7–9]

Mutations found in the genes for APP and the presenilins are major causes of familial early-onset AD (FAD) and commonly induce an increased ratio of Aβ42/40.[10–12] However, it is currently debatable whether this phenomenon results from a toxic gain of function by overproduction of Aβ42, or rather a partial loss-of-function mechanism leading to decreased generation of Aβ40.[13,14] Because of the limited availability of human neuronal tissue, most *in vitro* studies on APP processing have focused on heterologous overexpression systems involving mutant human APP_{695} and PS1.[4,5]

Here, we set out to study APP processing in human neurons generated *in vitro* from human embryonic stem cell (hESC)-derived and induced pluripotent stem cell (iPSC)-derived neural stem cells.[15] Neurons generated from these cells endogenously express APP_{695} as well as β- and γ-secretases. They show efficient processing of endogenous APP and secretion of Aβ. Importantly, the production of Aβ can be modulated using pharmacologically active compounds. We further demonstrate that the FAD-associated $PS1_{L166P}$ mutation results in elevated Aβ42/40 ratio caused by a selective decrease in Aβ40 production, supporting a partial loss of function in γ-secretase activity in this AD variant.

Materials and Methods

Cell Culture

The derivation of long-term self-renewing neuroepithelial-like stem cells (lt-NES cells) from human pluripotent stem cells has been performed as described previously.[15,16] The human ES cell line I3 was provided by Joseph Itskovitz-Eldor and Michal Amit (Technion, Israel Institute of Technology, Haifa, Israel). The cells (derived from hESC lines I3 as well as iPSC line PKa) were cultured on plastic dishes coated with polyornithin/laminin (both from Sigma-Aldrich, St. Louis, MO) in Dulbecco's modified Eagle's/F12 medium supplemented with N2 (high transferrin, T1129, 2005) (PAA Laboratories, Pasching, Austria) and containing 10 ng/mL basic fibroblast growth factor 2 (FGF2), 10 ng/mL epidermal growth factor (EGF) (both from R&D Systems, Minneapolis, MN), and 1:1000 B-27 Supplement (Invitrogen, Carlsbad, CA). Cells were passaged every 3 to 4 days at a 1:2 to 1:3 ratio using trypsin/EDTA. Replating densities were 30% to 40%. Differentiation was initiated by plating the cells on plastic dishes coated with Matrigel (BD Biosciences, San Jose, CA) and omission of growth factors. Differentiation medium was composed of Dulbecco's modified Eagle's/F12 medium supplemented with N2 (PAA Laboratories) and neurobasal medium supplemented with B-27 (Life Technologies, Grand Island, NY) mixed at a 1:1 ratio. Nonessential amino acids, 0.8 mg/L glucose, and 300 ng/mL cAMP were added.

Vector Design and Lentiviral Transgenesis

The coding DNA sequences for $PS1_{wt}$, $PS1_{D385N}$, and $PS1_{L166P}$ were amplified by PCR and cloned into a lentiviral backbone between an elongation factor 1-α (EF1α) promoter and an internal ribosome entry site (IRES)–enhanced green fluorescent protein (EGFP) sequence. A vector expressing EGF only under control of the EF1α promoter was used as a control vector. Production of lentiviral particles was performed as described previously.[17] Briefly, HEK-293FT cells were cotransfected with the packaging plasmid psPAX2, the envelope plasmid pMD2.G, and the respective lentiviral vector plasmid (kind gift of Didier Trono). Viral particles were enriched by centrifugation, and lt-NES cells (originally derived from hESC line I3) were transduced, expanded for four to six passages and purified by fluorescence activated cell sorting (FACS) to yield homogenously EGFP-positive populations.

Immunofluorescence Analysis

For immunofluorescence analysis, cells were fixed in 4% paraformaldehyde, washed in PBS, and then blocked with 10% fetal calf serum in the presence of 0.1% Triton X-100 in PBS. Primary antibodies were applied overnight at 4°C. Secondary antibodies (Cy3-linked goat anti-mouse and fluorescein isothiocyanate–linked goat anti-rabbit; 1:250; Jackson ImmunoResearch/Dianova, Hamburg, Germany) were applied for 2 hours at room temperature, and cell nuclei were counterstained with DAPI (Sigma-Aldrich). Antibodies used for immunofluorescence analysis are listed in Table 1.[18–21]

Treatment of Neuronal Cultures with γ-Secretase Modulators

Cells were cultured in the presence of either 250 μmol/L ibuprofen (Alexis Biochemicals, San Diego, CA), 100 μmol/L indomethacin (Cayman Chemical Company, Ann Arbor, MI), or ethanol (0.1%) as a solvent control for 24 hours. Cell pellets were used to determine total protein levels, and supernatants were subjected to enzyme-linked immunosorbent assay (ELISA) measurements.

Aβ Measurements by ELISA

Secreted Aβ peptides in conditioned medium were quantified by a sandwich immunoassay using the Meso Scale

Table 1. Primary Antibodies

Antibody	Source	Dilution
Immunocytochemical analysis		
APP	Chemicon/4G8	1:1000
Nestin	R&D Systems/MAB1259	1:800
MAP2ab	Chemicon/MAB378	1:500
GABA	Sigma-Aldrich/A2052	1:500
GFAP	DAKO/ZO334	1:1000
Presenilin-1	GeneTex/APS18	1:300
GFP	Abcam/ab296	1:3000
Beta III-tubulin	Covance/Tuj1	1:3000
Beta III-tubulin	BAbCo/MM5435P	1:1500
Sox2	R&D Systems	1:300
Western		
Presenilin-1	Raised/3109[18]	1:500
Full-length APP	Raised/140[19]	1:500
APP-CTF	Raised/140[19]	1:500
Soluble APP	Raised/5313[20]	1:1000
BACE1	Raised/7520[21]	1:1000
Actin	Sigma-Aldrich	1:2000
Nicastrin	Sigma-Aldrich	1:2000
Abeta	Signet/6E10	1:1000
Beta-III tubulin	Covance/TuJ1	1:1000

Discovery Sector Imager 2400 (Meso Scale Discovery Sector, Gaithersburg, MD) as described previously.[4] Briefly, streptavidin-coated 96-well multiarray plates were incubated with biotinylated 2D8 capture antibody. This was followed by addition of media samples and Aβ peptide standards (Bachem, Bubendorf, Switzerland). Ruthenylated C-terminal–specific anti-Aβ40 or anti-Aβ42 antibodies were used as detection antibodies. For detection, Meso Scale Discovery Read buffer was added, and the light emission at 620 nm after electrochemical stimulation was measured using the Meso Scale Discovery Sector Imager 2400 reader. The corresponding concentrations of Aβ peptides were calculated using the Meso Scale Discovery Workbench software and normalized to total cellular protein levels of the corresponding cell pellets.

Protein Sample Preparation and Western Blot Analysis

Cellular proteins were detected by Western blot analysis either in isolated membrane extracts or total cell lysates. For isolating cellular membranes, cells were scraped from the dishes and incubated in hypotonic buffer [10 mmol/L Tris (pH 7.3), 10 mmol/L $MgCl_2$, 1 mmol/L EDTA, 1 mmol/L EGTA] for 10 minutes on ice. Cells were then homogenized by using a 21-gauge needle and centrifuged for 10 minutes at 300 × g to pellet nuclei. The resulting supernatant was centrifuged for 30 minutes at 16,100 × g to obtain the membrane fraction as a pellet. Total cell lysates were obtained by lysis of cells in STEN buffer [50 mmol/L Tris (pH 7.6), 150 mmol/L NaCl, 2 mmol/L EDTA] supplemented with 1% NP-40, 1% Triton X-100, 2% bovine serum albumin on ice for 10 minutes. Lysates were clarified by centrifugation for 20 minutes at 16,100 × g. Membrane and whole lysate proteins were separated by SDS-PAGE and subsequently transferred to a nitrocellulose membrane (Schleicher & Schuell BioScience, Keene, NH). Respective proteins were detected by immunoblotting using appropriate antibodies and enhanced chemiluminescence reagent ECL (Amersham Pharmacia Biotech, Little Chalfont, UK). Antibodies used for Western blot are listed in Table 1. For detection of Aβ by Western blotting Aβ was immunoprecipitated from conditioned medium for 12 hours at 4°C using polyclonal antibody 2964[19] and protein A-sepharose (PAS) beads.

Immunoprecipitation and Immunoblot Analysis of Aβ Length Variants

For the separation of Aβ length variants, Aβ peptides were immunoprecipitated from conditioned medium mixed with a fivefold concentrated immunoprecipitation detergent buffer yielding final concentrations of 50 mmol/L HEPES, 150 mmol/L NaCl, 0.5% Nonidet P-40 v/v, 0.25% sodium deoxycholate w/v, 0.05% SDS w/v, and 25 μL of activated magnetic beads (antibody 1E8, 40 μg/mL, 15 hours at 4°C; Nanotools, Teningen, Germany). Beads were washed 3× (PBS/0.1% bovine serum albumin w/v) and 1× [10 mmol/L Tris-HCl (pH 7.5)], eluted by boiling in sample buffer (0.36 mol/L bis-Tris, 0.16 mol/L Bicine, 1% SDS w/v, 15% sucrose w/v, and 0.0075% bromphenol blue w/v), and then loaded on a urea-containing Bicine/bis-Tris/Tris/sulfate SDS-PAGE gel.[22] Separated Aβ peptides were transferred onto Immobilon-P polyvinylidene difluoride membranes (Millipore, Billerica, MA), detected with the 1E8 antibody (Nanotools) and visualized using a biotinylated anti-mouse IgG secondary antibody (Vector Laboratories, Linaris, Germany), a streptavidin–horseradish peroxidase complex (GE Healthcare, Little Chalfont, UK) and the ECL-plus substrate (GE Healthcare).

Semiquantitative and Quantitative RT-PCR Analysis

RNA from cells was purified using RNeasy kit (Qiagen, Valencia, CA) and subsequent DNaseI digestion (Life Technologies). cDNAs were generated using the iScript cDNA synthesis kit (Bio-Rad, Hercules, CA). Semiquantitative RT-PCR was performed using TaqDNA Polymerase (Invitrogen), with omission of cDNA serving as a negative control. cDNA from RNA extracts of human fetal or adult brains (Stratagene, Agilent Technologies, Santa Clara, CA) was used as positive controls. Quantitative real-time RT-PCR (RT-qPCR) analyses were performed in triplicates on a Bio-Rad iCycler using the SYBR Green detection method. PCR products were assessed by dissociation curve analysis. Data were normalized to GAPDH mRNA levels and analyzed using the ΔΔCt calculation method. Primers used are listed in Table 2.

Fluorescence Activated Cell Sorting

Lentivirally transduced It-NES cells were trypsinized, resuspended in Cytocoon Buffer II (Evotec, Hamburg, Germany) containing 0.1% DNase (Invitrogen) (3×10^6 cells/mL), and then filtered through a 40-μm nylon mesh (Pall GmbH, Dreieich, Germany). FACS was performed under

Table 2. Primer Sequences for RT-PCR Analysis

Name	Forward	Reverse
Semiquantitative RT-PCR		
APPtotal	5′-TGGCCCTGGAGAACTACATC-3′	5′-AATCACACGGAGGTGTGTCA-3′
APP exon15+	5′-TTGAGCCTGTTGATGCCCGC-3′	5′-CCACCACACCATGATGAATGGATG-3′
APP exon 7/8−	5′-GAGGTGGTTCGAGTTCCTACAACAGC-3′	5′-GGCTGCTTCCTGTTCCAAAGATTCCAC-3′
APP_{695}	5′-GAGGTGGTTCGAGTTCCTACAACAGC-3′	5′-AGGGCGGGCATCAACAGGCTCAA-3′
BACE1	5′-AGGCCATTCCCTGTAGGAGT-3′	5′-TTCCTGTCCTGGGAAAAATG-3′
BACE2	5′-TGTAGCCAGCAACTGTGTCC-3′	5′-ATTTCCAGCGATGTCTGACC-3′
Presenilin-1	5′-TGGTTGGTGAATATGGCAGA-3′	5′-GCGAGGATACTGCTGGAAAG-3′
Presenilin-2	5′-CATCTGAGGGACATGGTGTG-3′	5′-AAACCTGCTGTGCTTCCTGT-3′
Nicastrin	5′-GGGACATTAAAGCCTGACGA-3′	5′-CGAGCTGCCAATGTAGTCAA-3′
Aph1a	5′-GCATTTTTCTGGCTGGTCTC-3′	5′-AACCCCTCATCTGCCTTCTT-3′
Pen2	5′-CACCTCCTGGATCACCATCT-3′	5′-GGTCCTTTATTGGGGGATGT-3′
APLP1	5′-GAGTAGAGGGGGCTGAGGAC-3′	5′-CCAGGCATGCCAAAGTAAAT-3′
ApoE	5′-GGTCGCTTTTGGGATTACCT-3′	5′-TGTTCCTCCAGTTCCGATTT-3′
GAPDH	5′-CTGCTTTTAACTCTGGTAAAGT-3′	5′-GCGCCAGCATCGCCCCA-3′
Quantitative RT-PCR		
GAPDH	5′-CTGCTTTTAACTCTGGTAAAGT-3′	5′-GCGCCAGCATCGCCCA-3′
HES5	5′-GCACATTTGCCTTTTGTGAA-3′	5′-CACACTCAGGAGCCTTTTGG-3′

sterile conditions using a FACS DiVa sorter (BD Biosciences) equipped with an argon-ion laser (Coherent, Santa Clara, CA) operating at 488 nm. The desired cell populations were selected using the FACSDiva software (BD Biosciences) according to forward scatter, side scatter, and EGFP fluorescence.

BrdU Assay

Lt-NES cells (l3) were incubated with 5-bromo-2′-deoxyuridine (BrdU) (10 μmol/L final concentration; Sigma-Aldrich) for 3.5 hours at 37°C and subsequently fixed in 4% paraformaldehyde in PBS, washed in PBS, and permeabilized with 0.5% Triton X-100 for 30 minutes at room temperature. Cells were washed in PBS, treated with 2 N HCl for 10 minutes at room temperature for DNA denaturation and subsequently with 0.1 mol/L borate buffer for 10 minutes at room temperature. After three washes in PBS, cells were incubated for 30 minutes at room temperature with blocking solution (5% fetal calf serum, 0.1% Triton X-100 in PBS). Antibody staining and detection were performed as described for immunofluorescence analysis.

TUNEL Assay

Terminal deoxynucleotidyl transferase dUTP nick-end labeling (TUNEL) was performed to quantify apoptotic cells according to the manufacturer's instructions (Promega, Madison, WI).

Statistical Analyses

Quantitative data were generated in triplicate. Means and standard deviations were computed. All results presented as bar graphs show mean ± SD. Student's *t*-test was performed to determine whether a significant difference exists between groups ($^*P < 0.05$).

Results

Maturation-Dependent Expression of AD-Related Proteins and Amyloidogenic APP Processing in Human Embryonic Stem Cell–Derived Neurons

To investigate the proteolytic processing of APP in human neurons, we took advantage of our previously established population of lt-NES cells.[15,16] These cells can be propagated as a homogeneous population in the presence of the growth factors FGF2 and EGF while maintaining a strong and stable neurogenic differentiation potential. On growth factor withdrawal, lt-NES cells slowly differentiate into a major fraction of neurons and a minor fraction of glia (Figure 1A). Seven days after initiation of differentiation, the majority of the cells (94.0% ± 1.9%) still expressed the neural precursor marker nestin, whereas less than 6% of the cells acquired a neuronal morphology and expressed the neuronal marker β-III tubulin. By 14 days of differentiation, the number of neurons had increased to 9.2% ± 2.7% at the expense of the nestin-positive precursors. By 28 days, the cultures consisted of 78.0% ± 0.8% β-III tubulin–positive neurons and only 21.0% ± 0.7% nestin-positive cells (Figure 1A). At this point, about 30% of these nestin-positive cells coexpressed the astrocytic marker glial fibrillary acidic protein (GFAP) (data not shown). From 4 weeks onwards, the cultures remained largely stable as demonstrated by phase-contrast pictures and immunocytochemical analyses of neuronal and glial marker expression at 1 and 3 months after initiation of differentiation (see Supplemental Figure S1 at *http://ajp.amjpathol.org*). In parallel to the acquisition of a neuronal fate, expression of APP was detected in cells with neuronal morphology and increased with the number of β-III tubulin–positive cells (Figure 1A). By 4 weeks of differentiation, the vast majority of the β-III tubulin–positive neurons was strongly positive for APP (antibody 4G8), whereas the remaining stem

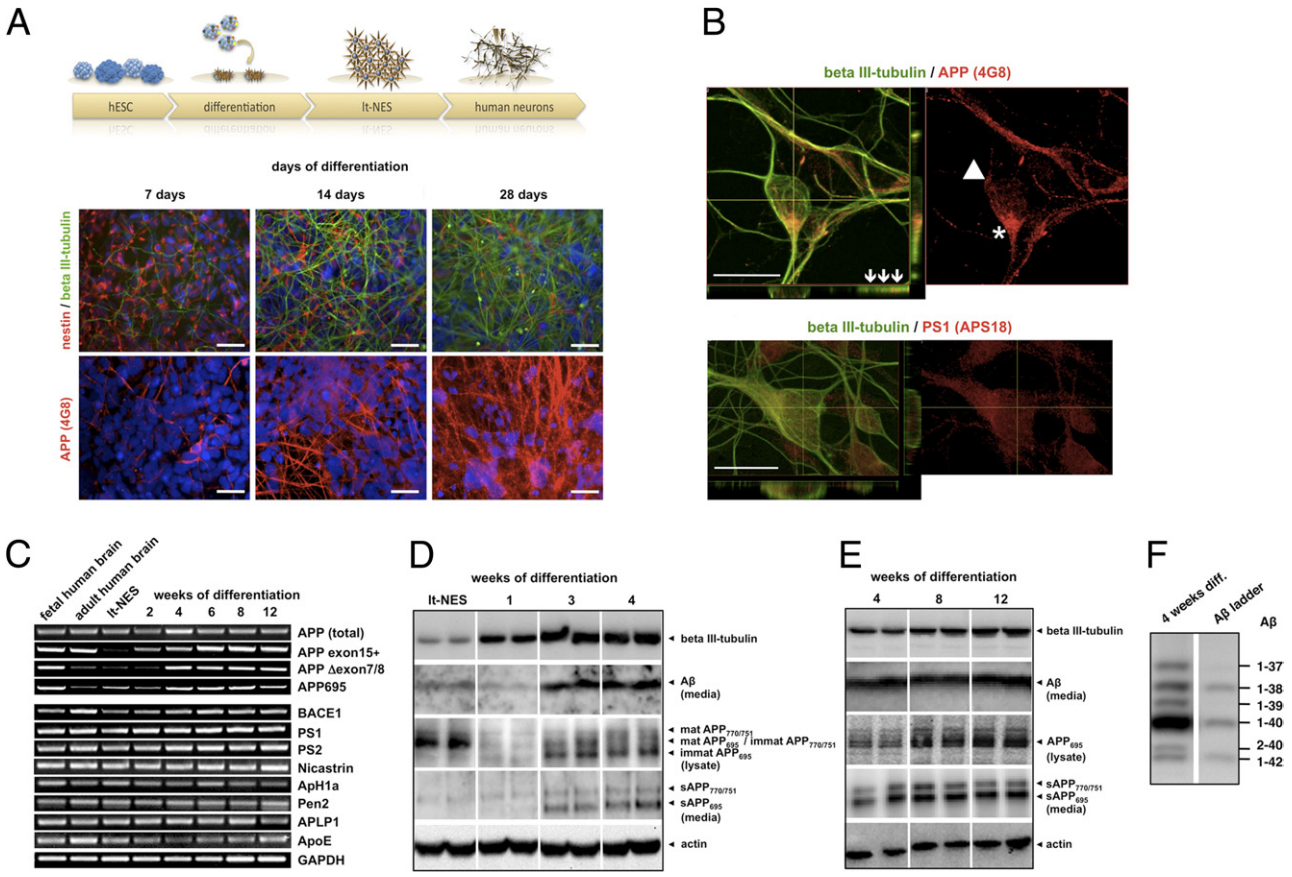

Figure 1. lt-NES cell–derived neurons express AD-associated proteins. **A:** Schematic overview showing the protocol for differentiation of pluripotent stem cells into postmitotic human neurons (**top**). Immunocytochemical analyses of nestin, β-III tubulin, and APP (antibody 4G8) in differentiating lt-NES cell cultures are also shown (**bottom**). Data are representative of three independent experiments per time point. **B:** Confocal immunocytochemical analysis of β-III tubulin, APP (antibody 4G8), and PS1 (antibody APS18) in 4 weeks differentiated neurons. **Arrows** indicate vesicle-like structures in axons, the **asterisk** marks axonal compartment, and the **triangle** indicates somatodendritic compartment. Data are representative of three independent experiments. **Lines** on the site depict digital reconstruction in different axes. **C:** RT-PCR analysis of APP variants, γ-secretase components, and other AD-related genes in differentiating cultures over time. Commercial total RNA samples from fetal and adult human brain served as controls. **D** and **E:** Western blot analysis of cells between 0 and 4 weeks (**D**) and 4 and 12 weeks (**E**) of differentiation. Immature (immat), mature (mat) APP (Antibody 140), and β-III tubulin were detected in cell lysates. Aβ (antibody 82E1) and soluble APP (sAPP; antibody 5313) were detected in conditioned media. Mature APP_{695} comigrates with the immature $APP_{770/751}$ isoforms of cell lysates, whereas the respective secreted forms of APP (sAPP) from conditioned media are clearly separated in SDS gels. **F:** Bicine/bis-Tris/Tris/sulfate SDS-PAGE separation of Aβ37, Aβ38, Aβ39, Aβ40, and Aβ42, as well as N-terminally truncated Aβ2–40, immunoprecipitated from conditioned media of neural cultures allowed to differentiate for 6 weeks. Scale bars: 50 μm (**A**); 20 μm (**B**).

and progenitor cells showed only weak staining. This pattern of APP expression reflects the *in vivo* situation in the developing mouse brain, as neural stem cells located in the ventricular zone show only very weak 4G8 staining, whereas newborn neurons that leave the ventricular zone and enter the cortical plate are strongly positive for 4G8 (see Supplemental Figure S2 at *http://ajp.amjpathol.org*). With increasing maturation, APP immunoreactivity also became more accentuated and localized in human lt-NES cell–derived neurons. In young neurons, APP was located throughout the perikaryon and neurites (Figure 1A). More mature neurons (6 weeks of differentiation) exhibited a pronounced axonal immunoreactivity at the expense of the somatodendritic compartment (Figure 1B). Within axons, the staining appeared dotty, which could be compatible with vesicular axonal transport known for APP. No such immunostaining was detected in cells positive for nestin or GFAP (data not shown). Neurons also showed a dotty cytoplasmic staining for PS1, which would be in accordance with a location within cytoplasmic vesicles and the endoplasmic reticulum (Figure 1B).

RT-PCR revealed mRNA expression of different AD-related proteins, including APP, BACE1, and the γ-secretase components PS1, PS2, Nicastrin, Aph1a, and Pen2 at all time points of differentiation (Figure 1C). In addition, APLP1 and apolipoprotein E (ApoE) mRNAs were detected. To assess alternative splicing of APP during neuronal differentiation, we performed RT-PCR analyses using variant-specific primers (Figure 1C). Undifferentiated lt-NES cells mainly expressed APP variants lacking exon 15, consistent with a preferential expression of these splice variants in non-neuronal cells.[23] On neuronal differentiation, the expression of exon 15–containing APP variants increased, indicating a shift toward neuron-specific splicing of APP in these cells. Notably, the neuron-specific APP_{695} mRNA isoform that lacks exons 7 and 8, and contains exon 15 increased after 4, 6, and 8 weeks of differentiation as compared to lt-NES cells, whereas total APP mRNA levels remained largely constant. (Figure 1C).

After 12 weeks, APP_{695} mRNA levels appeared to slightly decrease. Consistent with a previous report,[24] we also detected decreased levels of APP_{695} mRNA levels in adult human brain as compared to fetal human brain samples (Figure 1C). In line with the known alternative splicing of APP mRNA during neuronal differentiation,[25] we further noticed differentiation-dependent changes in the protein levels of cellular and secreted APP (sAPP) variants. We observed multiple bands in cell lysates, which are compatible with immature (*N*′-glycosylated) and mature (*N*′/*O*′-glycosylated) variants of the different APP isoforms. Undifferentiated lt-NES cells mainly expressed APP variants that represent immature $APP_{770/751}$ isoforms, as indicated by the comigration with endogenous $APP_{770/751}$ of HEK293 cells (Figure 1D; see also Supplemental Figure S3 at *http://ajp.amjpathol.org*). After 1 week of differentiation, expression of these variants strongly decreased. Notably, after 3 and 4 weeks differentiation, expression of the neuron-specific APP_{695} isoform increased as indicated by the appearance of a lower migrating variant in cell lysates and conditioned media (Figure 1D; see also Supplemental Figure S3 and S4 at *http://ajp.amjpathol.org*). The identity of the $sAPP_{695}$ variant is corroborated by comigration with a transgenic APP_{695} isoform expressed in HEK293 cells (see Supplemental Figure S3 at *http://ajp.amjpathol.org*). Together, these data indicate that neuronal differentiation of lt-NES cells is associated with the expression of the neuron-specific APP_{695} isoform.

The expression of two APP isoforms and their secretion into conditioned media was also observed on longer differentiation periods up to 12 weeks (Figure 1E). Most importantly, we also detected differentiation-dependent secretion of Aβ. Aβ levels were increased after 3 weeks of differentiation as compared to earlier time points (Figure 1, D and E; see also Supplemental Figure S4 at *http://ajp.amjpathol.org*). This increase coincided with the increased expression of the neuron-specific APP_{695} isoform. Increased expression of BACE1 as shown by RT-PCR might also contribute to elevated production of Aβ on differentiation (Figure 1C). As revealed by SDS-PAGE separation, several isoforms of Aβ, including Aβ37, Aβ38, Aβ39, Aβ40, and Aβ42, as well as N-terminally truncated Aβ2–40, were generated by the neurons (Figure 1F). Together, these data demonstrate that hESC-derived neurons endogenously express a neuron-specific pattern of APP as well as functional β- and γ-secretases, and produce different variants of Aβ.

Modulation of APP Processing by γ-Secretase Inhibition

We next explored whether proteolytic processing of APP can be pharmacologically modulated in hESC-derived neurons. Treatment of 4-week-differentiated cultures with the γ-secretase inhibitor *N*-[*N*-(3,5-difluorophenacetyl)-L-alanyl]-*S*-phenylglycine *t*-butyl ester (DAPT) efficiently inhibited the secretion of endogenous Aβ (10 μmol/L; 2 days; Figure 2A). Consistent with the inhibition of γ-secretase, DAPT treatment for 2 to 6 days led to a strong accumulation of APP C-terminal fragments (CTFs), which represent the immediate substrates for γ-secretase, whereas levels of full-length APP increased only slightly over a 6-day treatment time (Figure 2B). TUNEL analysis showed no significant differences in the number of TUNEL-positive nuclei of DAPT-treated cells as com-

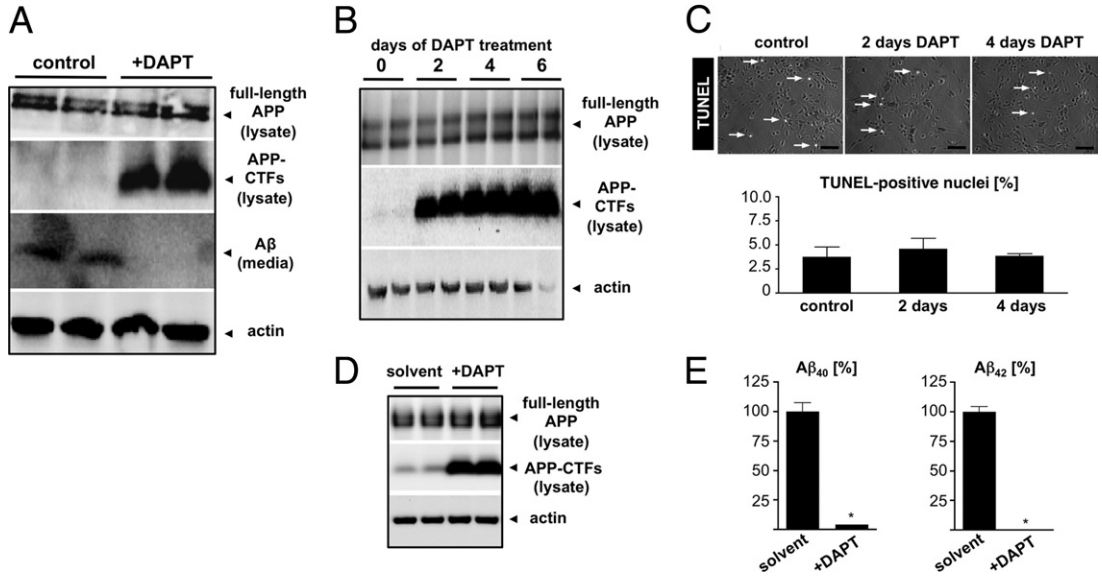

Figure 2. Endogenous APP processing and γ-secretase modulation in hESC- and iPSC-derived neurons. **A:** Immunoblot analysis of cellular full-length APP, APP-CTFs, and secreted Aβ of 4 weeks differentiated hESC-derived neurons with and without treatment with DAPT (10 μmol/L; 48 hours). **B:** Immunoblot showing full-length APP and APP-CTFs during prolonged treatment with DAPT (2, 4, and 6 days). Blots from A and B show biological duplicates and are representative of three independent experiments. **C:** TUNEL assay at 0, 2, and 4 days of DAPT treatment ($n = 3$ per group). TUNEL-positive nuclei (white) are marked by **arrows**. Quantification is shown below. **D:** Immunoblot analysis of neurons derived from human iPSC-derived lt-NES cells (differentiated for 4 weeks) with and without treatment with DAPT. Blots show biological duplicates and were performed in three independent experiments. **E:** ELISA analysis of Aβ40 and Aβ42 in conditioned media of iPSC-derived neurons treated with DAPT. Bar graphs throughout figure show mean ± SD of each group. $^*P < 0.05$.

pared to a vehicle-treated (dimethyl sulfoxide) control population (4.6% ± 1.1% or 3.9% ± 0.2% for cells treated for 2 or 4 days, respectively, versus 3.8% ± 1.0% in the control) and had no effect on cell morphology (Figure 2C).

Functional APP Processing in Induced Pluripotent Stem Cell–Derived Neurons

Recently, the derivation of iPSC derived from adult skin fibroblasts has become possible.[26] These cells, which can also be recruited from patients with familial and sporadic forms of AD, might be a valuable tool to study endogenous processing of APP and PS1 or APP mutations. We thus wondered whether our observations on APP processing can be recapitulated in neurons generated from human iPSC generated by retroviral transduction of adult skin fibroblasts with the reprogramming factors Oct4, Sox2, Klf4, and c-Myc. IPSC generated from a healthy donor expressed pluripotency markers, including alkaline phosphatase, Nanog, Tra1-60, and Tra1-81, showed sustained silencing of the transduced transgenes, and were capable of differentiating into derivates of all three germ layers (data not shown). Using the same differentiation protocol used for hESC,[15] these cells were successfully differentiated into iPSC-derived lt-NES cells homogeneously expressing nestin and Sox2. Western blot analyses performed after 4 weeks of growth factor withdrawal–induced differentiation showed that iPSC-derived neurons express full-length APP (Figure 2D). Comparable to hESC-derived neurons, strong accumulation of APP-CTFs was observed on treatment with DAPT (10 μmol/L, 48 h; Figure 2D). Further, as shown by ELISA measurement of conditioned medium, secretion of both Aβ40 and Aβ42 was strongly reduced by DAPT treatment (Figure 2E). These data suggest that modeling and modulation of proteolytic APP processing established in hESC-derived neuronal cultures can be translated to neurons differentiated from human iPSC.

Modulation of APP Cleavage by NSAIDs

NSAIDs were described to modulate the activity and cleavage specificity of γ-secretase toward lower Aβ42/40 ratios.[27] To evaluate the effect of NSAIDs on hESC-derived neurons, we treated cultures differentiated for 4 weeks with ibuprofen (250 μmol/L) and indomethacin (100 μmol/L), and analyzed Aβ levels in the supernatants. Both drugs reduced the secretion of Aβ42, whereas the secretion of Aβ40 was not significantly changed. This led to a reduction of the Aβ42/40 ratio with both drugs (reduction by 19% for indomethacin-treated and 22% for ibuprofen-treated cells; Figure 3).

Expression of a PS1 FAD Mutant Results in a Partial Loss of γ-Secretase Function

Mutations in the presenilin genes are a major cause of FAD. Several studies indicate that these mutations alter the γ-secretase–dependent proteolytic processing of APP-CTFs, thereby increasing the ratios of Aβ42/40.[28] Among the different mutants, the $PS1_{L166P}$ variant is a very aggressive form, resulting in an onset of symptoms already during the second decade of life.[29] To model the effects of FAD-mutant PS1 in human neural cells, we lentivirally transduced proliferating hESC-derived lt-NES cells to express $PS1_{L166P}$ and, as controls, wild-type PS1 ($PS1_{wt}$) or a catalytically inactive variant $PS1_{D385N}$. Expression was driven by the EF1α promoter and linked to an EGFP sequence by an internal ribosome entry site (IRES; Figure 4A). Transduction efficiencies ranged from 39% to 60%. To obtain homogeneous populations of neural stem cells expressing the individual forms of PS1, the transduced cells were expanded for four to six passages and subsequently purified by FACS for EGFP expression. This resulted in homogeneous populations of cells expressing nestin and Sox2 in >98% of EGFP-positive cells (Figure 4B). To exclude detrimental effects of lentiviral transduction and FACS sorting on lt-NES cells, we transduced lt-NES cells with the same vector carrying EGFP only and sorted for green fluorescence. Direct comparison of non-transduced cells and EGFP-transduced cells revealed that both populations exhibit comparable marker expression and proliferation capacity (see Supplemental Figure S5 at *http://ajp.amjpathol.org*).

Immunostaining for PS1 (antibody APS18) and EGFP confirmed overexpression of the different PS1 variants (Figure 4B), which was stable for at least 15 passages

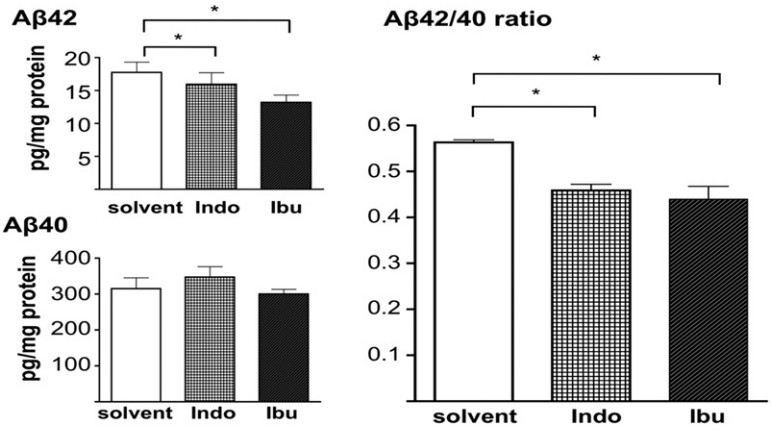

Figure 3. Modulation of γ-secretase activity by nonsteroidal anti-inflammatory drugs (NSAIDs). ELISA measurement of Aβ40 and Aβ42 in conditioned media of neurons differentiated for 4 weeks with and without treatment with indomethacin (Indo; 100 μmol/L) or ibuprofen (Ibu; 250 μmol/L). ELISA measurements were performed as biological and technical triplicates, and the Aβ42/40 ratio was calculated (**right**). Bar graphs show mean ± SD of each group. $^*P < 0.05$.

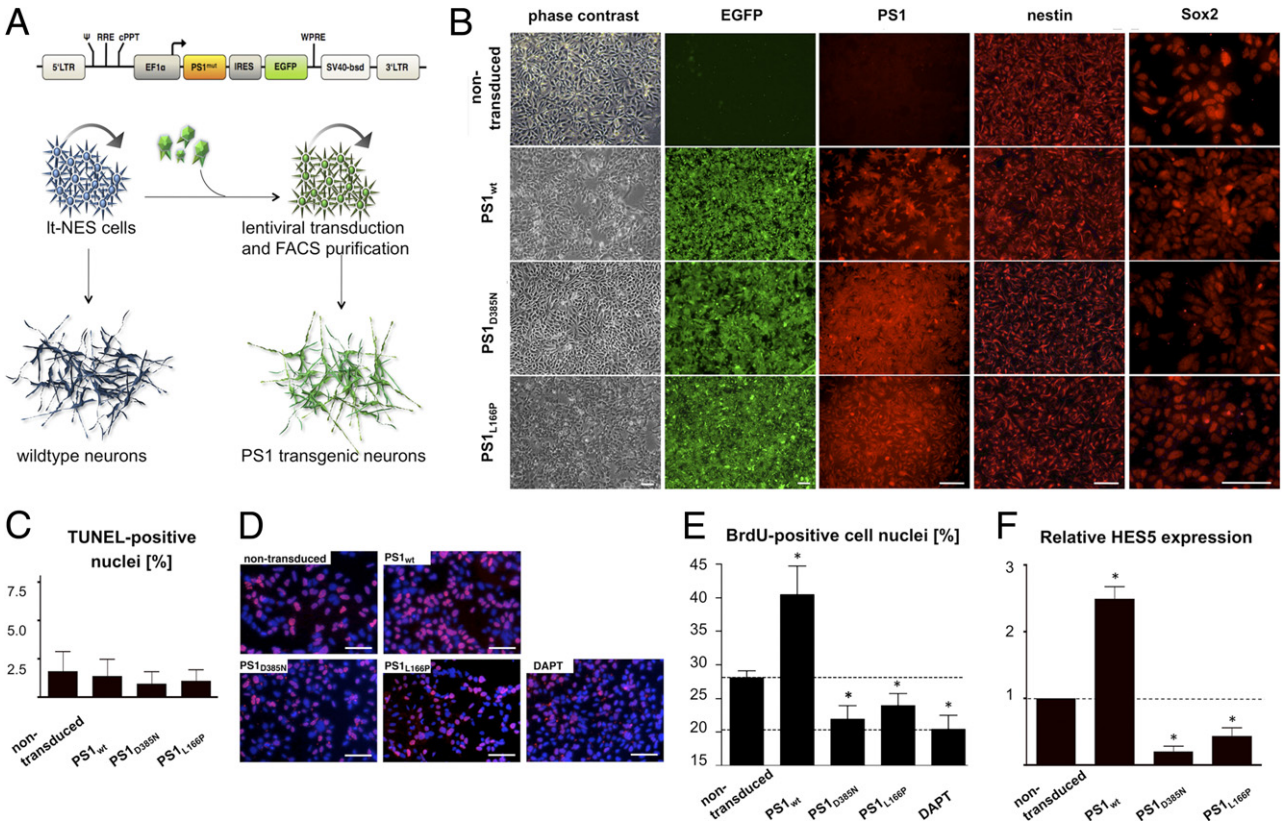

Figure 4. Stable lentiviral PS1 transgenesis in neural stem cells. **A:** Schematic showing the lentiviral construct and overview of the experimental design. Human lt-NES cells were infected with lentiviral vectors encoding PS1 (wt, D385N, and L166P) and EGFP. Green fluorescent cells were purified by FACS sorting and further cultured as transgenic lt-NES cells. On withdrawal of growth factors, transgenic lines give rise to cultures of human neurons overexpressing the different PS1 variants. **B:** Immunocytochemical analysis of PS1, EGFP, nestin, and Sox2 of different lt-NES cell lines. Data are representative of two independent experiments. **C:** TUNEL assay of proliferating lt-NES cell lines overexpressing $PS1_{wt}$, $PS1_{D385N}$, or $PS1_{L166P}$ ($n = 3$ per group). **D:** BrdU incorporation assay of proliferating transgenic and DAPT-treated lt-NES cells in the absence of the mitogen FGF2 ($n = 3$ per group). BrdU-incorporated nuclei are stained in red. Nuclei are counterstained with DAPI. **E:** Quantification of BrdU incorporation assay. **F:** Quantitative real-time RT-PCR expression analysis of the Notch1 responsive HES5 transcript in lt-NES cell lines overexpressing $PS1_{wt}$, $PS1_{D385N}$, or $PS1_{L166P}$. Experiments were performed as biological and technical triplicates. Bar graphs throughout figure show mean ± SD of each group. $^*P < 0.05$. Scale bars: 50 μm (**B** and **D**).

(data not shown). We next investigated whether mutated PS1 had an influence on cell proliferation and survival. TUNEL staining revealed that 1.7% ± 1.3% of the non-transduced cells, 1.4% ± 1.1% of $PS1_{wt}$, 0.9% ± 0.8 of $PS1_{L166P}$, and 1.1% ± 0.8 of $PS1_{D385N}$ cells were TUNEL-positive, indicating that overexpression of the different PS1 isoforms did not induce apoptosis in this experimental setting (Figure 4C). In neural stem cells, including lt-NES cells, γ-secretase activity has been described as essential for maintaining Notch signaling, activation of Notch target genes such as *HES5*, and cell proliferation.[30] We therefore analyzed the influence of $PS1_{wt}$ and mutated PS1 overexpression on proliferation of lt-NES cells. To that end, we quantified BrdU incorporation in the different lt-NES cell lines in the absence of the mitogen FGF2 following a 3.5-hour pulse (Figure 4D). In the non-transduced group, 28.1% ± 1.1% of the cells were positive for BrdU. This number increased by 44% to 40.1% ± 4.3% in the $PS1_{wt}$-transduced cells, indicating a proproliferative effect of $PS1_{wt}$ overexpression. Overexpression of the inactive $PS1_{D385N}$ variant significantly reduced the number of BrdU-positive lt-NES cells (21.9% ± 2.0%) similar to Notch blockade by DAPT treatment (20.4% ± 2.1%). The reduction in BrdU incorporation in $PS1_{D385N}$-overexpressing cells could be explained by dominant-negative effects of this mutant, because it suppresses the incorporation of endogenous functional PS1 into the γ-secretase complex. Neural stem cells overexpressing $PS1_{L166P}$ showed a marked decrease of BrdU-positive nuclei to 24.0% ± 1.8%, indicating that this disease-associated mutant also exerts a slight dominant-negative effect on the S3 cleavage of Notch (Figure 4, D and E). In accordance with increased FGF2-independent proliferation, RT-qPCR analysis for the immediate Notch target gene HES5 of lt-NES cells overexpressing $PS1_{wt}$ showed 2.5-fold elevated HES5 levels, whereas the transcript levels in $PS1_{D385N}$ and $PS1_{L166P}$ cells were significantly decreased (Figure 4F).

We next studied whether the overexpression of the different PS1 variants remains stable during neuronal differentiation. To that end, the transgenic lt-NES cell lines were differentiated by growth factor withdrawal for 4 weeks, and the expression of neural markers, as well as EGFP and PS1, was analyzed by immunocytochemistry. Cultures transduced with the different lentiviral constructs showed strong EGFP expression in cells with neuronal and glial morphology (Figure 5A). At the same time, PS1 transgenic lines stained intensively positive for PS1,

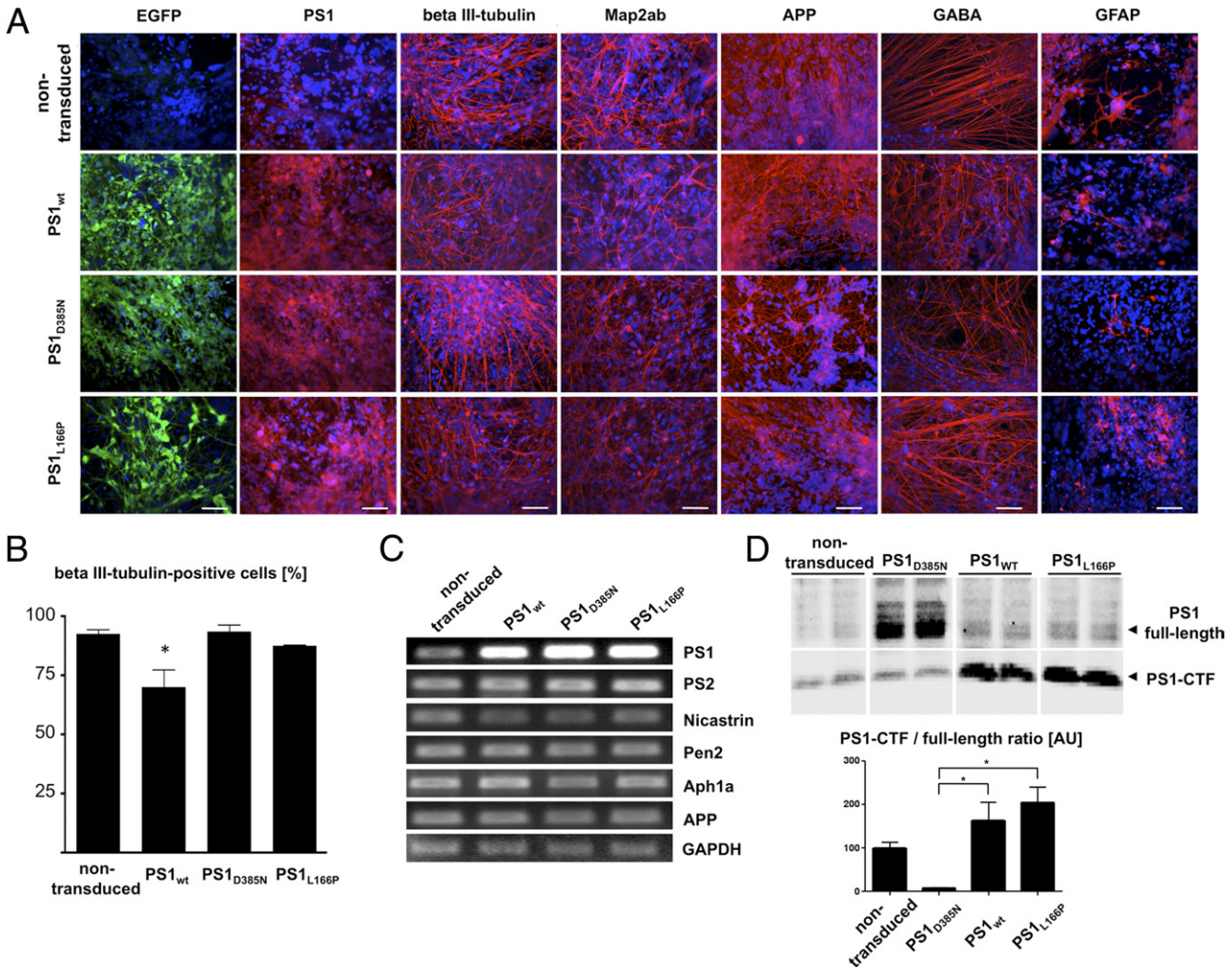

Figure 5. Characterization of human neurons overexpressing PS1 variants. **A:** Neuronal cultures differentiated for 4 weeks immunostained for EGFP and PS1, as well as β-III tubulin, MAP2ab, APP, GABA, and GFAP. Data are representative of two independent experiments. **B:** Quantitative analysis of the number of β-III tubulin–positive neurons in differentiated lt-NES cells ($n = 3$ per group). Bar graph shows mean ± SD of each group. $^*P < 0.05$. **C:** RT-PCR analysis shows expression of APP, PS1, and other γ-secretase genes in 4 weeks differentiated neurons. Results shown are representative for three independent experiments. **D:** Immunoblot for PS1 and PS1-CTF of transgenic neurons in comparison to nontransduced controls. Bar graph shows quantification by densitometric analysis of PS1-CTFs to full-length PS1 (mean ± SD of each group. $^*P < 0.05$). Scale bars: 50 μm (**A**).

whereas non-transduced cells showed only a weak staining of the endogenously expressed protein (Figure 5A). Quantification of the β-III tubulin–positive and MAP2ab-positive cells revealed that all four populations contained comparable numbers of neurons following 4 weeks of differentiation (Figure 5B). Only in the case of $PS1_{wt}$-overexpressing cells we observed a slight reduction of the relative numbers of neurons, which was associated with an increased number of cells still expressing nestin and could point to a prolonged growth factor–independent proliferation, presumably due to a constitutive activation of the Notch pathway.[30] The number of GFAP-positive cells remained constantly below 10% in all four populations. Consistent with our previous results, lt-NES cells mainly gave rise to GABAergic neurons,[15] a property that was not affected by PS1 overexpression (Figure 5A). RT-PCR analysis revealed strongly increased mRNA levels of PS1 in transduced cells (Figure 5C). PS2 mRNA was not changed indicating that mRNA expression of PS2 is not affected by overexpression of PS1. APP and other γ-secretase components (Nicastrin, Pen2, and Aph1a) were also expressed at comparable levels (Figure 5C). Immunoblotting revealed that both $PS1_{wt}$ and $PS1_{L166P}$ undergo endoproteolytic processing, resulting in increased levels of the CTFs. By contrast, cells expressing the $PS1_{D385N}$ mutant showed strong accumulation of the full-length protein and induced a slight decrease in endogenous CTFs as compared to control cells, which is in agreement with the notion that the $PS1_{D385N}$ mutant does not undergo endoproteolytic processing and suppresses the incorporation of endogenous PS1 protein into the γ-secretase complex in a dominant-negative fashion (Figure 5D).[31] Together, these data demonstrate that overexpressed $PS1_{wt}$ and $PS1_{L166P}$ are endoproteolytically processed, whereas the $PS1_{D385N}$ variant accumulates as a nonprocessed full-length protein.

To assess the functional implication of the respective PS1 variants in the proteolytic processing of APP in human neurons, the secretion of Aβ isoforms was analyzed

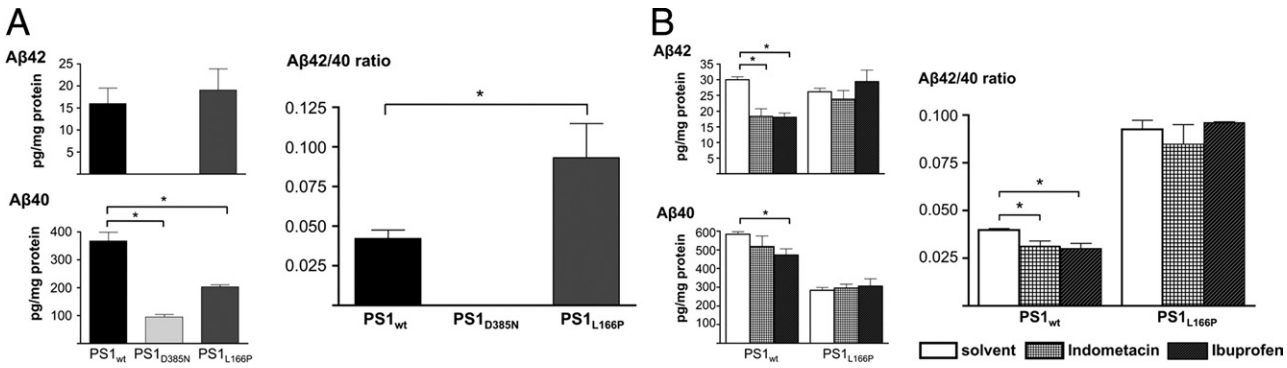

Figure 6. HESC-derived neurons transduced with PS1 mutants show altered Aβ generation. **A:** ELISA measurement of Aβ40 and Aβ42 in conditioned media of $PS1_{wt}$, $PS1_{D385N}$, or $PS1_{L166P}$ transgenic neurons differentiated for 4 weeks. **B:** ELISA of Aβ40 and Aβ42 in conditioned media of indomethacin- and ibuprofen-treated neurons overexpressing $PS1_{wt}$, $PS1_{D385N}$, or $PS1_{L166P}$. All ELISA measurements were performed as biological and technical triplicates, and the Aβ42/40 ratio was calculated (**right** of each panel). Bar graphs show mean ± SD of each group. $^*P < 0.05$.

in 4-week-differentiated cultures by ELISA. Compared to $PS1_{wt}$-expressing cells, $PS1_{D385N}$ expression resulted in strong reduction in the secretion of Aβ40, and Aβ42 secretion dropped below the detection limit of the assay (Figure 6A). Importantly, in comparison to $PS1_{wt}$-expressing control neurons, cells expressing the $PS1_{L166P}$ variant showed a selective decrease in the secretion of Aβ40, whereas secretion of Aβ42 was similar to that of $PS1_{wt}$-expressing cells. As a consequence, the Aβ42/40 ratio was strongly elevated, indicating that $PS1_{L166P}$ acts via a partial loss in Aβ40 production, which results in strongly altered Aβ42/40 ratios (Figure 6A). A similar effect was observed when in parallel to ELISA measurements, Aβ species were analyzed by SDS-PAGE separation (see Supplemental Figure S6 at *http://ajp.amjpathol.org*). To assess whether treatment with NSAIDs affects Aβ production in FAD-mutated neurons, we treated $PS1_{wt}$- or $PS1_{L166P}$-overexpressing cultures with NSAIDs for 36 hours. Notably, neither indomethacin nor ibuprofen had a significant impact on the secretion of Aβ42 or Aβ40 from endogenous wild-type APP in $PS1_{L166P}$-overexpressing cells, whereas Aβ42 was markedly decreased in $PS1_{wt}$-overexpressing cultures (Figure 6B). This is in line with previous findings, as some FAD-associated PS1 mutations appear to be insensitive to these γ-secretase modulators.[4,5]

Discussion

In the study of disease-associated mechanisms, cell culture models can provide useful tools, supplementing postmortem studies and animal models. This is particularly true for neurodegenerative diseases, as access to primary tissue is limited, and murine models do not always reflect the human pathological phenotype at a molecular level.[32,33] The issue of species specificity is also relevant for Alzheimer's disease, where processing of APP has been found to be highly species- and cell type–specific.[25,34] The Aβ domain of human APP differs from its murine homologue by three amino acids at positions 5, 10, and 13, which strongly affects its proteolytic processing by β-secretase. As compared to the human variants, murine APP is processed very inefficiently to Aβ.[35] A human neuronal cell system should thus provide significant advantages for studying the production of Aβ from endogenously expressed APP.

Human pluripotent stem cells are supposed to provide particularly promising prospects for human disease modeling as they can be used to generate cells of all three germ layers in unlimited quantities, including neurons.[15,32] The *in vitro* generation of bulk numbers of human neurons largely facilitates biochemical studies, which, due to limited access, cannot be conducted using primary tissue. The results of our study show that both hESC- and iPSC-derived neurons endogenously express major AD-associated proteins and efficiently process APP. Moreover, this *in vitro* system responds to known pharmacological modulators of γ-secretase, including DAPT and NSAIDs. Using lentiviral overexpression of the FAD-associated mutation $PS1_{L166P}$, we further demonstrate that this cell culture system can be used to address pathophysiological changes in familial monogenic forms of the disease.

APP Processing in Human Neuronal Cultures

Many existing cellular AD models are based on the overexpression of the human neuronal isoform APP_{695} in non-neuronal cells. By contrast, hESC-derived neurons endogenously express different splice variants of APP, including the neuron-specific 695 amino acid–long variant. In these neurons, APP also undergoes physiological sorting as immunocytochemical detection revealed polarized axonal localization very similar to the *in vivo* condition. Most importantly, our neuronal culture system exhibits functional amyloidogenic APP processing with endogenous secretion of different Aβ length variants into the cell culture medium. Although mRNA expression of BACE1 appeared to slightly increase with neuronal maturation, expression of the critical γ-secretase component PS1 was largely unchanged during neuronal differentiation. Moreover, mRNA expression levels of other γ-secretase components including Nicastrin, Aph-1, and Pen-2 were also not significantly changed during prolonged *in vitro* differentiation of human neurons. Thus, the increased production of Aβ in "older" hESC-derived neurons is likely caused by increased protein levels of

APP_{695} and probably also of BACE1, rather than increased expression of γ-secretase components.

Modulation of APP Processing by Small Molecules: Proof of Principle for Cellular Assays

The treatment of hESC and iPSC lt-NES cell–derived neurons with the known γ-secretase inhibitor DAPT efficiently led to strongly decreased production of Aβ from endogenous APP and to the simultaneous accumulation of APP-CTFs, thereby confirming expression of a functional γ-secretase complex. Thus, modulation of disease-associated pathways by pharmacological substances can be monitored in mature lt-NES cell–derived neurons. Epidemiological data suggest that prolonged use of NSAIDs, which target cyclooxygenase (COX), a key mediator of the inflammatory cascade, for conditions like arthritis, entails a reduced risk and delayed onset of AD.[36,37] Initially, the effect of NSAIDs on AD was attributed to a reduction of inflammation.[38] It was also reported that a subset of NSAIDs selectively reduced Aβ42 production in cultured cells and in the mouse brain independent of COX inhibition, but rather by directly affecting the cleavage of APP-CTFs by γ-secretase or directly targeting APP-CTFs.[27,39,40] We tested the influence of the NSAIDs ibuprofen and indomethacin on the proteolytic processing of endogenously expressed APP in hESC-derived neurons. Both drugs proved to be functional and significantly reduced the Aβ42/40 ratio in these cells, demonstrating that lt-NES cell–derived neuronal cultures are suitable for assessing the impact of applied small molecular drugs on endogenous APP processing. Translated to a multiwell format, the analysis of Aβ42/40 ratios should enable cell-based screening for additional small molecules, which impact on the production and processing of APP in human neurons.

Modeling of FAD-Associated PS1 Mutation in lt-NES Cells and Derived Neurons Reveals Partial Loss of γ-Secretase Function

The stability of lt-NES cells and their constant neurogenic potential enabled us to stably overexpress PS1 variants in lt-NES cells and their neuronal progeny. $PS1_{wt}$ or the FAD-associated $PS1_{L166P}$ mutant underwent endoproteolytic processing to stable N-terminal and C-terminal fragments that represent components of active γ-secretase complexes, whereas $PS1_{D385N}$ accumulated as an unprocessed full-length protein.

Overexpression of $PS1_{wt}$ stimulated the proliferation of lt-NES cells, likely via increased Notch signaling.[30] On the contrary, expression of the catalytically inactive $PS1_{D385N}$ variant, as well as the FAD-associated $PS1_{L166P}$ variant, reduced proliferation in the absence of FGF2, which goes in line with reduced levels of HES5 expression in these cells. Thus, overexpression of $PS1_{L166P}$, very similar to the catalytically inactive $PS1_{D385N}$ variant, appears to decrease the capacity to activate the Notch signaling pathway in lt-NES cells. These data are consistent with previous reports that this mutation impairs γ-secretase–dependent processing of Notch and nuclear translocation of the Notch intracellular domain in non-neuronal cells.[29,41]

In postmitotic neurons, overexpression of $PS1_{wt}$ led to a significantly increased secretion of Aβ40 and Aβ42 variants, thereby demonstrating the activity of transgenic $PS1_{wt}$. By contrast, expression of the $PS1_{D385N}$ variant strongly decreased the secretion of both Aβ variants, confirming efficient suppression of endogenous γ-secretase activity in a dominant-negative fashion. Importantly, in comparison to $PS1_{wt}$, neurons expressing the FAD-associated $PS1_{L166P}$ mutant showed a strongly reduced secretion of Aβ40. By contrast, the secretion of Aβ42 by $PS1_{L166P}$-transgenic neurons was very similar to that of their $PS1_{wt}$-transduced counterparts. Thus, the strongly increased Aβ42/40 ratio in the $PS1_{L166P}$ mutant appears to be due to a partial loss of function in Aβ40 generation rather than an increased production of the more aggregation-prone Aβ42 variant. These data support the view that FAD-linked mutations in PS1 can lead to a partial loss of its physiological functions, such as Aβ40 generation or the S3 cleavage of Notch, whereas other γ-secretase processes are unaffected, as for example, Aβ42 generation is not attenuated by the L166P mutation.[13,14,42] The overexpression of different PS1 variants in lt-NES cells allowed the comparison of their activities in the same genetic background. However, it will be interesting to study APP processing and Aβ generation also in PS1 FAD patient-derived iPSC neurons that express a mutant and wild-type PS allele at the endogenous levels.

Recent data suggest that Aβ40 might decrease plaque formation *in vivo*.[43] Thus, it will be interesting to assess whether decreased levels of Aβ40 could promote the aggregation of Aβ42 and thereby increase neurotoxicity of Aβ species produced by PS1 FAD mutant cells. Taken together, our data demonstrate that hESC- and iPSC-derived stem cell–derived lt-NES cells and their neuronal progeny represent suitable cellular models for studying the expression and metabolism of AD-associated proteins and for assessing AD-related cytopathological processes. Bypassing nonphysiological expression levels typically associated with transgenic approaches, as well as cell type and/or species-specificity problems encountered with heterologic expression systems, pluripotent stem cell–derived neurons might prove particularly valuable as a platform for the development and testing of novel pharmaceutical compounds.

Acknowledgments

We thank Dr. Konrad Beyreuther for monoclonal antibody APS18, Dr. Christian Haass for providing antibody AB5313, Dr. Lodovica Borghese for advice on gene expression analysis, Anna Kabanova for providing E12.5 brain sections, and Dr. Elmar Endl (Flow Cytometry Facility, University Hospital Bonn) for cell sorting. We are grateful to Svenja Auel and David Kühne for excellent technical support. We thank Drs. Joseph Itskovitz-Eldor and Michal Amit (Technion, Israel Institute of Technology, Haifa, Israel) for providing the human ES cell line I3 used to derive the lt-NES cells used in this study.

References

1. Selkoe DJ: Alzheimer's disease: genes, proteins, and therapy. Physiol Rev 2001, 81:741–766
2. Walter J, Kaether C, Steiner H, Haass C: The cell biology of Alzheimer's disease: uncovering the secrets of secretases. Curr Opin Neurobiol 2001, 11:585–590
3. Cole SL, Vassar R: BACE1 structure and function in health and Alzheimer's disease. Curr Alzheimer Res 2008, 5:100–120
4. Page RM, Baumann K, Tomioka M, Perez-Revuelta BI, Fukumori A, Jacobsen H, Flohr A, Luebbers T, Ozmen L, Steiner H, Haass C: Generation of Abeta38 and Abeta42 is independently and differentially affected by familial Alzheimer disease-associated presenilin mutations and gamma-secretase modulation. J Biol Chem 2008, 283:677–683
5. Czirr E, Cottrell BA, Leuchtenberger S, Kukar T, Ladd TB, Esselmann H, Paul S, Schubenel R, Torpey JW, Pietrzik CU, Golde TE, Wiltfang J, Baumann K, Koo EH, Weggen S: Independent generation of Abeta42 and Abeta38 peptide species by gamma-secretase. J Biol Chem 2008, 283:17049–17054
6. Takami M, Nagashima Y, Sano Y, Ishihara S, Morishima-Kawashima M, Funamoto S, Ihara Y: gamma-Secretase: successive tripeptide and tetrapeptide release from the transmembrane domain of beta-carboxyl terminal fragment. J Neurosci 2009, 29: 13042–13052
7. Haass C, Selkoe DJ: Soluble protein oligomers in neurodegeneration: lessons from the Alzheimer's amyloid beta-peptide. Nat Rev Mol Cell Biol 2007, 8:101–112
8. Hardy J, Selkoe DJ: The amyloid hypothesis of Alzheimer's disease: progress and problems on the road to therapeutics. Science 2002, 297:353–356
9. De Strooper B, Vassar R, Golde T: The secretases: enzymes with therapeutic potential in Alzheimer disease. Nat Rev Neurol 2010, 6:99–107
10. Citron M, Westaway D, Xia W, Carlson G, Diehl T, Levesque G, Johnson-Wood K, Lee M, Seubert P, Davis A, Kholodenko D, Motter R, Sherrington R, Perry B, Yao H, Strome R, Lieberburg I, Rommens J, Kim S, Schenk D, Fraser P, St George Hyslop P, Selkoe DJ: Mutant presenilins of Alzheimer's disease increase production of 42-residue amyloid beta-protein in both transfected cells and transgenic mice. Nat Med 1997, 3:67–72
11. Borchelt DR, Thinakaran G, Eckman CB, Lee MK, Davenport F, Ratovitsky T, Prada CM, Kim G, Seekins S, Yager D, Slunt HH, Wang R, Seeger M, Levey AI, Gandy SE, Copeland NG, Jenkins NA, Price DL, Younkin SG, Sisodia SS: Familial Alzheimer's disease-linked presenilin 1 variants elevate Abeta1-42/1–40 ratio in vitro and in vivo. Neuron 1996, 17:1005–1013
12. Scheuner D, Eckman C, Jensen M, Song X, Citron M, Suzuki N, Bird TD, Hardy J, Hutton M, Kukull W, Larson E, Levy-Lahad E, Viitanen M, Peskind E, Poorkaj P, Schellenberg G, Tanzi R, Wasco W, Lannfelt L, Selkoe D, Younkin S: Secreted amyloid beta-protein similar to that in the senile plaques of Alzheimer's disease is increased in vivo by the presenilin 1 and 2 and APP mutations linked to familial Alzheimer's disease. Nat Med 1996, 2:864–870
13. Shen J, Kelleher RJ, 3rd: The presenilin hypothesis of Alzheimer's disease: evidence for a loss-of-function pathogenic mechanism, Proc Natl Acad Sci U S A 2007, 104:403–409
14. De Strooper B: Loss-of-function presenilin mutations in Alzheimer disease. Talking point on the role of presenilin mutations in Alzheimer disease. EMBO Rep 2007, 8:141–146
15. Koch P, Opitz T, Steinbeck JA, Ladewig J, Brüstle O: A rosette-type, self-renewing human ES cell-derived neural stem cell with potential for in vitro instruction and synaptic integration. Proc Natl Acad Sci U S A 2009, 106:3225–3230
16. Falk A, Koch P, Kesavan J, Takashima Y, Ladewig J, Alexander M, Wiskow O, Tailor J, Trotter M, Pollard S, Smith A, Brüstle O: Capture of neuroepithelial-like stem cells from pluripotent stem cells provides aversatile system for in vitro production of human neurons. PLoS One 2012, 7:e29597
17. Koch P, Siemen H, Biegler A, Itskovitz-Eldor J, Brüstle O: Transduction of human embryonic stem cells by ecotropic retroviral vectors. Nucleic Acids Res 2006, 34:e120
18. Prager K, Wang-Eckhardt L, Fluhrer R, Killick R, Barth E, Hampel H, Haass C, Walter J. A structural switch of presenilin 1 by glycogen synthase kinase 3beta-mediated phosphorylation regulates the interaction with beta-catenin and its nuclear signaling. J Biol Chem 2007, 282:14083–14093
19. Wahle T, Thal DR, Sastre M, Rentmeister A, Bogdanovic N, Famulok M, Heneka MT, Walter J. GGA1 is expressed in the human brain and affects the generation of amyloid beta-peptide. J. Neurosci 2006, 26:12838–12846
20. Walter J, Capell A, Hung AY, Langen H, Schnölzer M, Thinakaran G, Sisodia SS, Selkoe DJ, Haass C. Ectodomain phosphorylation of beta-amyloid precursor protein at two distinct cellular locations. J Biol Chem 1997, 272:1896–1903
21. Capell A, Steiner H, Willem M, Kaiser H, Meyer C, Walter J, Lammich S, Multhaup G, Haass C. Maturation and pro-peptide cleavage of beta-secretase. J Biol Chem 275, 30849–30854
22. Wiltfang J, Esselmann H, Bibl M, Smirnov A, Otto M, Paul S, Schmidt B, Klafki HW, Maler M, Dyrks T, Bienert M, Beyermann M, Ruther E, Kornhuber J: Highly conserved and disease-specific patterns of carboxyterminally truncated Abeta peptides 1–37/38/39 in addition to 1–40/42 in Alzheimer's disease and in patients with chronic neuroinflammation. J Neurochem 2002, 81:481–496
23. Bergsdorf C, Paliga K, Kreger S, Masters CL, Beyreuther K: Identification of cis-elements regulating exon 15 splicing of the amyloid precursor protein pre-mRNA. J Biol Chem 2000, 275:2046–2056
24. O'Hara BF, Fisher S, Oster-Granite ML, Gearhart JD, Reeves RH: Developmental expression of the amyloid precursor protein, growth-associated protein 43, and somatostatin in normal and trisomy 16 mice. Brain Res Dev Brain Res 1989, 49:300–304
25. Hung AY, Koo EH, Haass C, Selkoe DJ: Increased expression of beta-amyloid precursor protein during neuronal differentiation is not accompanied by secretory cleavage, Proc Natl Acad Sci U S A 1992, 89:9439–9443
26. Takahashi K, Tanabe K, Ohnuki M, Narita M, Ichisaka T, Tomoda K, Yamanaka S: Induction of pluripotent stem cells from adult human fibroblasts by defined factors. Cell 2007, 131:861–872
27. Weggen S, Eriksen JL, Das P, Sagi SA, Wang R, Pietrzik CU, Findlay KA, Smith TE, Murphy MP, Bulter T, Kang DE, Marquez-Sterling N, Golde TE, Koo EH: A subset of NSAIDs lower amyloidogenic Abeta42 independently of cyclooxygenase activity. Nature 2001, 414:212–216
28. Sisodia SS, St George-Hyslop PH: gamma-Secretase. Notch, Abeta and Alzheimer's disease: where do the presenilins fit in? Nat Rev Neurosci 2002, 3:281–290
29. Moehlmann T, Winkler E, Xia X, Edbauer D, Murrell J, Capell A, Kaether C, Zheng H, Ghetti B, Haass C, Steiner H: Presenilin-1 mutations of leucine 166 equally affect the generation of the Notch and APP intracellular domains independent of their effect on Abeta 42 production. Proc Natl Acad Sci U S A 2002, 99:8025–8030
30. Borghese L, Dolezalova D, Opitz T, Haupt S, Leinhaas A, Steinfarz B, Koch P, Edenhofer F, Hampl A, Brüstle O: Inhibition of notch signaling in human embryonic stem cell-derived neural stem cells delays G1/S phase transition and accelerates neuronal differentiation in vitro and in vivo. Stem Cells 2010, 28:955–964
31. Wolfe MS, Xia W, Ostaszewski BL, Diehl TS, Kimberly WT, Selkoe DJ: Two transmembrane aspartates in presenilin-1 required for presenilin endoproteolysis and gamma-secretase activity. Nature 1999, 398: 513–517
32. Koch P, Kokaia Z, Lindvall O, Brüstle O: Emerging concepts in neural stem cell research: autologous repair and cell-based disease modelling. Lancet Neurol 2009, 8:819–829
33. Wichterle H, Przedborski S: What can pluripotent stem cells teach us about neurodegenerative diseases? Nat Neurosci 2010, 13: 800–804
34. Fung J, Frost D, Chakrabartty A, McLaurin J: Interaction of human and mouse Abeta peptides. J Neurochem 2004, 91:1398–1403
35. De Strooper B, Simons M, Multhaup G, Van Leuven F, Beyreuther K, Dotti CG: Production of intracellular amyloid-containing fragments in hippocampal neurons expressing human amyloid precursor protein and protection against amyloidogenesis by subtle amino acid substitutions in the rodent sequence. EMBO J 1995, 14:4932–4938
36. Etminan M, Gill S, Samii A: Effect of non-steroidal anti-inflammatory drugs on risk of Alzheimer's disease: systematic review and meta-analysis of observational studies. BMJ 2003, 327:128
37. Sastre M, Walter J, Gentleman SM: Interactions between APP secretases and inflammatory mediators. J Neuroinflammation 2008, 5:25

38. McGeer PL, McGeer EG: NSAIDs and Alzheimer disease: epidemiological, animal model and clinical studies. Neurobiol Aging 2007, 28:639–647
39. Kukar TL, Ladd TB, Bann MA, Fraering PC, Narlawar R, Maharvi GM, Healy B, Chapman R, Welzel AT, Price RW, Moore B, Rangachari V, Cusack B, Eriksen J, Jansen-West K, Verbeeck C, Yager D, Eckman C, Ye W, Sagi S, Cottrell BA, Torpey J, Rosenberry TL, Fauq A, Wolfe MS, Schmidt B, Walsh DM, Koo EH, Golde TE: Substrate-targeting gamma-secretase modulators. Nature 2008, 453:925–929
40. Eriksen JL, Sagi SA, Smith TE, Weggen S, Das P, McLendon DC, Ozols VV, Jessing KW, Zavitz KH, Koo EH, Golde TE: NSAIDs and enantiomers of flurbiprofen target gamma-secretase and lower Abeta 42 in vivo. J Clin Invest 2003, 112:440–449
41. Bentahir M, Nyabi O, Verhamme J, Tolia A, Horre K, Wiltfang J, Esselmann H, De Strooper B: Presenilin clinical mutations can affect gamma-secretase activity by different mechanisms. J Neurochem 2006, 96:732–742
42. Tamboli IY, Prager K, Thal DR, Thelen KM, Dewachter I, Pietrzik CU, St George-Hyslop P, Sisodia SS, De Strooper B, Heneka MT, Filippov MA, Muller U, van Leuven F, Lutjohann D, Walter J: Loss of gamma-secretase function impairs endocytosis of lipoprotein particles and membrane cholesterol homeostasis. J Neurosci 2008, 28:12097–12106
43. Kim J, Onstead L, Randle S, Price R, Smithson L, Zwizinski C, Dickson DW, Golde T, McGowan E: Abeta40 inhibits amyloid deposition in vivo. J Neurosci 2007, 27:627–633